JOC*Article*

Prediction of the ^{1}H and ^{13}C NMR Spectra of α-D-Glucose in Water by DFT Methods and MD Simulations

Alessandro Bagno,[†] Federico Rastrelli,[†] and Giacomo Saielli*,[‡]

Dipartimento di Scienze Chimiche, Università di Padova, via Marzolo, 1-35131 Padova, Italy, and Istituto per la Tecnologia delle Membrane del CNR, Sezione di Padova, via Marzolo, 1-35131 Padova, Italy

giacomo.saielli@unipd.it

Received May 29, 2007

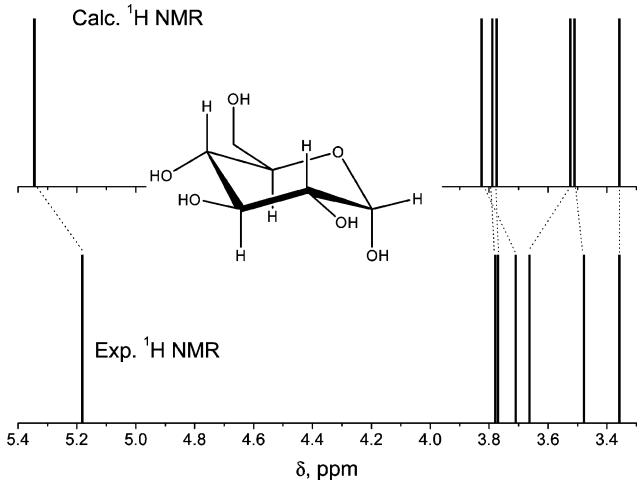

We have applied computational protocols based on DFT and molecular dynamics simulations to the prediction of the alkyl ^{1}H and ^{13}C chemical shifts of α-D-glucose in water. Computed data have been compared with accurate experimental chemical shifts obtained in our laboratory. ^{13}C chemical shifts do not show a marked solvent effect. In contrast, the results for ^{1}H chemical shifts provided by structures optimized in the gas phase are only fair and point out that it is necessary to take into account both the flexibility of the glucose structure and the strong effect exerted by solvent water thereupon. Thus, molecular dynamics simulations were carried out to model both the internal geometry as well as the influence of solvent molecules on the conformational distribution of the solute. Snapshots from the simulation were used as input to DFT NMR calculations with varying degrees of sophistication. The most important factor that affects the accuracy of computed ^{1}H chemical shifts is the solute geometry; the effect of the solvent on the shielding constants can be reasonably accounted for by self-consistent reaction field models without the need of explicitly including solvent molecules in the NMR property calculation.

Introduction

NMR has become a staple methodology for the determination of the molecular structure of newly synthesized molecules, intermediates, or species obtained from natural sources. Despite the steady advancement in NMR techniques, these may not lead to an unambiguous structure. This is especially true of natural substances, which continue to supply organic chemists with a fascinating variety of intricate structures and unusual functionalities. There is, therefore, a genuine need for tools to accurately predict NMR spectra.

One might approach the problem by database lookup; however, if the species of interest has uncommon structural features, its viability must be validated. On the other hand, DFT methods have indeed enabled the computation of NMR parameters[1] with good accuracy even for naturally occurring complex

[†] Università di Padova.
[‡] ITM-CNR, Sezione di Padova.

(1) Kaupp, M., Bühl, M., Malkin V. G., Eds. *Calculation of NMR and EPR Parameters*; Wiley-VCH: Weinheim, Germany, 2004.
(2) Bagno, A.; Saielli, G. *Theor. Chem. Acc.* **2007**, *117*, 603.
(3) Bagno, A.; Rastrelli, F.; Saielli, G. *Chem.—Eur. J.* **2006**, *12*, 5514.

10.1021/jo071129v CCC: $37.00
Published on Web 08/24/2007

molecules.[2−8] Our studies were mostly restricted to conformationally rigid, weakly polar molecules;[3,9,10] obviously, many organic molecules do not fit these requirements.

Dealing with flexibility introduces significant complications because one has to identify all relevant conformers, weighting them according to a Boltzmann distribution, or resort to molecular dynamics (MD) simulations to let the system sample the accessible space.[5b,d,11]

Dealing with solvent effects also leads to difficulties because solvation affects NMR parameters through changes in the solute geometry and electronic structure or through direct solute−solvent interactions.[12,13] These effects can be approached by means of continuum or explicit methods, each having their own advantages and shortcomings. We previously found that a continuum solvent method such as PCM, despite its simplified modeling and modest computational cost, allows the correct trends in spectral parameters to be induced.[3,14] Recent trends have favored the inclusion of explicit solvent molecules and their dynamics, often by computing NMR parameters on snapshots of molecular dynamics simulations.[15−17] With this approach, we showed that it is possible to predict the anion effect on the ^{1}H and ^{13}C spectra of imidazolium-based ionic liquids, where solute−solvent interactions are strong, long-ranged, and complex.[18,19]

Carbohydrates occupy a special place among natural substances, owing to their widespread occurrence, varied structure, and stereochemistry; however, their characterization by NMR is still difficult.[20] Notably, carbohydrates embody all the above problematic characteristics and offer unique opportunities to probe the limitations of DFT NMR calculations.

Among carbohydrates, there is hardly any doubt that glucose plays an outstanding role; at the same time, it features all the "undesirable" properties listed above. (a) Aqueous solutions undergo mutarotation, leading to a mixture of α and β anomers with overlapping NMR spectra, thereby hampering long experiments. (b) Most nonexchangeable protons lie in rather similar chemical environments and therefore give rise to a crowded, and sometimes not even first-order, spectrum which may be difficult to interpret; in fact, ^{1}H signals (except the anomeric proton) fall within a narrow range of 0.8 ppm, and two signals are even accidentally almost isochronous (see below). (c) Most importantly, OH groups are located in such a way that intramolecular hydrogen bonding is conceivable, but this situation is likely to be overturned by solvent. Conversely, only the cyclic pyranose form is important (at variance with other monosaccharides).[21] In this work, we present the calculation of α-D-glucose ^{1}H and ^{13}C chemical shifts through a combination of MD runs and DFT calculations.

SCHEME 1. Structural Formula of α-D-Glucopyranose (the O5−C5−C6−O6 dihedral angle of the hydroxymethylene group (ϕ) is highlighted)

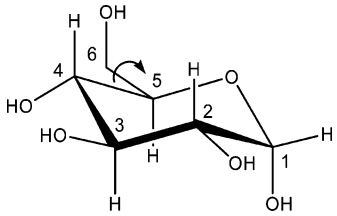

Results

The potential energy surface of simple carbohydrates has been studied by means of molecular mechanics,[22] semiempirical, DFT,[23] and ab initio methods.[24−27] α-D-Glucose (Scheme 1) has been investigated in detail.[26,27] As a general picture, in the gas phase, an intramolecular chain of hydrogen bonds is established between hydroxyl groups at C1−C4, which may be arranged in a clockwise (cw) or counterclockwise (ccw) fashion, the latter being more stable. However, this intramolecular network can be expected to be disrupted by a solvent such as water; there seems to be no evidence of persistent intramolecular hydrogen bonds in water.[28]

Concerning the arrangement of the hydroxymethylene group, three rotamers exist which differ by the value of the O5−C5−C6−O6 dihedral angle ϕ: gauche−gauche (*gg*, $\phi = 60°$), gauche−trans (*gt*, $\phi = -60°$), and trans−gauche (*tg*, $\phi = 180°$). According to the above studies, their relative stability is *tg* > *gg* > *gt*.

In contrast with the stability in the gas phase, the relative stability of the three rotamers in water at room temperature, as

(4) Meiler, J.; Sanli, E.; Junker, J.; Meusinger, R.; Lindel, T.; Will, M.; Maier, W.; Köck, M. *J. Chem. Inf. Comput. Sci.* **2002**, *42*, 241.
(5) (a) Barone, G.; Gomez-Paloma, L.; Duca, D.; Silvestri, A.; Riccio, R.; Bifulco, G. *Chem.—Eur. J.* **2002**, *8*, 3233. (b) Barone, G.; Duca, D.; Silvestri, A.; Gomez-Paloma, L.; Riccio, R.; Bifulco, G. *Chem.—Eur. J.* **2002**, *8*, 3240. (c) Cimino, P.; Gomez-Paloma, L.; Duca, D.; Riccio, R.; Bifulco, G. *Magn. Reson. Chem.* **2004**, *42*, S26. (d) Cimino, P.; Bifulco, G.; Evidente, A.; Abouzeid, M.; Riccio, R.; Gomez-Paloma, L. *Org. Lett.* **2002**, *4*, 2779. (e) Bifulco, G.; Bassarello, C.; Riccio, R.; Gomez-Paloma, L. *Org. Lett.* **2004**, *6*, 1025. (f) Bifulco, G.; Gomez-Paloma, L.; Riccio, R.; Gaeta, C.; Troisi, F.; Neri, P. *Org. Lett.* **2005**, *7*, 5757.
(6) (a) Colombo, D.; Ferraboschi, P.; Ronchetti, F.; Toma, L. *Magn. Reson. Chem.* **2002**, *40*, 581. (b) Aiello, A.; Fattorusso, E.; Luciano, P.; Mangoni, A.; Menna, M. *Eur. J. Org. Chem.* **2005**, 5024.
(7) Trost, B. M.; Harrington, P. E. *J. Am. Chem. Soc.* **2004**, *126*, 5028.
(8) Rychnovsky, S. D. *Org. Lett.* **2006**, *8*, 2895.
(9) Bagno, A. *Chem.—Eur. J.* **2001**, *7*, 1652.
(10) Bagno, A.; Rastrelli, F.; Saielli, G. *J. Phys. Chem. A* **2003**, *107*, 9964.
(11) Tähtinen, P.; Bagno, A.; Klika, K. D.; Pihlaja, K. *J. Am. Chem. Soc.* **2003**, *125*, 4609.
(12) Bagno, A.; Rastrelli, F.; Saielli, G. *Prog. Nucl. Magn. Reson. Spectrosc.* **2005**, *47*, 41.
(13) Aidas, K.; Møgelhøj, A.; Kjær, K.; Nielsen, C. B.; Mikkelsen, K. V.; Ruud, K.; Christiansen, O.; Kongsted, J. *J. Phys. Chem. A* **2007**, *111*, 4199.
(14) Bagno, A.; Bonchio, M.; Autschbach, J. *Chem.—Eur. J.* **2006**, *12*, 8460.
(15) Bühl, M.; Grigoleit, S.; Kabrede, H.; Mauschick, F. T. *Chem.—Eur. J.* **2006**, *12*, 477.
(16) Pavone, M.; Brancato, G.; Morelli, G.; Barone, V. *ChemPhysChem* **2006**, *7*, 148.
(17) Komin, S.; Gossens, C.; Tavernelli, I.; Rothlisberger, U.; Sebastiani, D. *J. Phys. Chem. B* **2007**, *111*, 5225.
(18) Bagno, A.; D'Amico, F.; Saielli, G. *J. Phys. Chem. B* **2006**, *110*, 23004.
(19) Bagno, A.; D'Amico, F.; Saielli, G. *ChemPhysChem* **2007**, *8*, 873.
(20) Duus, J. O.; Gottfredsen, C. H.; Bock, K. *Chem. Rev.* **2000**, *100*, 4589.
(21) Zhu, Y.; Zajicek, J.; Serianni, A. S. *J. Org. Chem.* **2001**, *66*, 6244.
(22) Dowd, M. K.; French, A. D.; Reilly, P. J. *Carbohydr. Res.* **1994**, *1*, 264.
(23) Cramer, C. J.; Truhlar, D. G. *J. Am. Chem. Soc.* **1993**, *115*, 5745.
(24) Glennon, T. M.; Zheng, Y.; LeGrand, S. M.; Shutzberg, B. A.; Merz, K. M., Jr. *J. Comput. Chem.* **1994**, *15*, 1019.
(25) (a) Henry-Ryad, H.; Tang, T.-H.; Csizmadia, I. G. *J. Mol. Struct. (THEOCHEM)* **1999**, *492*, 67. (b) Guler, L. P.; Yu, Y.-Q.; Kenttämaa, H. *J. Phys. Chem. A* **2002**, *106*, 6754. (c) French, A. D.; Johnson, G. P.; Kelterer, A.-M.; Dowd, M. K.; Cramer, C. J. *J. Phys. Chem. A* **2002**, *106*, 4988.
(26) Brown, J. W.; Wladkowski, B. D. *J. Am. Chem. Soc.* **1996**, *118*, 1190.
(27) Ma, B.-Y.; Schaefer, H. F., III; Allinger, N. L. *J. Am. Chem. Soc.* **1998**, *120*, 3411.
(28) Adams, B.; Lerner, L. *J. Am. Chem. Soc.* **1992**, *114*, 4827.

determined by ^{1}H NMR, is *gg* (ca. 60%) > *gt* (ca. 40%) ≫ *tg* (negligible).[29] Indeed, recent estimates of the relative stability of the gas-phase rotamers at 298 K agree with the *gt* and *gg* conformers being the most stable ones.[30] The effect of solvation has been investigated in detail[31] using the ASEP/MD method, which iteratively alternates molecular dynamics simulation and quantum mechanics calculation. The main conclusion of that work was that the relative stability of the various conformers is significantly affected by the solvent. In qualitative agreement with the experiment, the *tg* conformer was destabilized in water compared to *gg* and *gt*.

Nevertheless, since the differences in energy are rather small, a quantitative description of the equilibrium distribution of the conformers of α-D-glucose in solution at a QM level remains a formidable task. This is due on one hand to the large number of conformations of the glucose hydroxyl groups, which, in water, are not arranged neither in the counterclockwise nor in the clockwise fashion but rather form strong hydrogen bonds with water molecules; on the other hand, the solvation shell itself may have an almost continuum distribution of configurations and long-range electrostatic solvent effects also play a role.[32]

Classical molecular dynamics simulations largely reduce the computational cost and allow one to treat the solvent explicitly, both in its structure and dynamics, but they are limited by the approximate nature of the force fields employed. Indeed, a ground-breaking simulation of glucose in water with the Car−Parrinello scheme was limited to a few picoseconds;[33] more recent first-principles MD simulations have reached a time scale 1 order of magnitude longer.[34,35] Systems with strong solute−solvent interactions have been also described by first-principles MD simulations,[36] as well as cases where electronic effects on the dynamics are relevant.[37] Nevertheless, classical MD simulations represent the only route available to describe solvent effects in systems where slow (nanosecond time scale) conformational dynamics, such as *gauche/trans* transitions about a dihedral angle, take place.

Although other force fields designed for carbohydrates have been presented,[38] recently an improved force field for carbohydrates in water has been developed[39] which qualitatively reproduces the correct population of rotamers in solution.

We have employed this force field to generate an MD trajectory which served as a source of configurations for QM calculations of ^{1}H and ^{13}C chemical shifts. It is well-known that the NMR properties of a solute molecule are very sensitive probes of the environment.[12] It is also now known that a rather high accuracy in the calculation of ^{1}H and ^{13}C chemical shifts can be attained by using DFT methods, about 0.1 and 1 ppm for $\delta(^1\text{H})$ or $\delta(^{13}\text{C})$, respectively.[2] Therefore, by running DFT calculations on the structures obtained from the simulation and comparing the results with those obtained from the gas-phase-optimized structures, one expects to understand the solvent effects of water on the alkyl proton and carbon chemical shifts.

TABLE 1. ^{1}H and ^{13}C Experimental Chemical Shifts of α-D-Glucose in D_2O at 298 K[a]

atom no.	$\delta(^1\text{H})$ ppm	$\delta(^{13}\text{C})$ ppm
1	5.182	92.48
2	3.478	71.87
3	3.664	73.15
4	3.358	70.04
5	3.77[b]	71.82
6a[c]	3.711	60.99
6b[c]	3.78[b]	

[a] See Experimental Section for details. [b] As obtained from an HSQC spectrum at 301 K. [c] Assigned on the basis of ref 29.

An extensive ab initio and DFT study of ^{13}C chemical shifts of a series of saccharides has been reported recently[40] where solvent effects were accounted for by continuum and cluster models but without considering the dynamics of the system. However, it was found that none of the solvent models employed were fully successful. On the other hand, a variety of saccharides has been the object of computational works aimed at modeling the spin−spin coupling constants (J_{CC}, J_{CH}, and J_{HH}) observable in such molecules.[41−45]

NMR Spectra. ^{1}H and ^{13}C experimental chemical shifts are reported in Table 1. Our results are in agreement with previously reported data.[29,46] ^{1}H chemical shifts were obtained from the "proton-decoupled proton spectrum" that results from projecting a tilted and symmetrized *J*-resolved spectrum on the direct dimension. In the context of *J*-resolved spectroscopy, it is well-known that strong coupling leads to the appearance of misleading extra signals which are commonly referred to as "artifacts" despite them being authentic and predictable on a formal basis. However, when *J*-modulation is achieved by means of a double rather than a single spin−echo, the symmetry of these extra signals is broken in such way that a simple postprocessing scheme leads in most cases to an efficient quenching of the unwanted artifacts.[47] Nonetheless, the aforementioned strategy fails to resolve chemical shifts when very strong coupling

(29) (a) Nishida, Y.; Ohrui, H.; Meguro, H. *Tetrahedron Lett.* **1984**, *25*, 1575. (b) Nishida, Y.; Hori, H.; Ohrui, H.; Meguro, H. *J. Carbohydr. Chem.* **1988**, *7*, 239.
(30) Barrows, S. E.; Storer, J. W.; Cramer, C. J.; French, A. D.; Truhlar, D. G. *J. Comput. Chem.* **1998**, *19*, 1111.
(31) Corchado, J. C.; Sanchez, M. L.; Aguilar, M. A. *J. Am. Chem. Soc.* **2004**, *126*, 7311.
(32) da Silva, C. O.; Mennucci, B.; Vreven, T. *J. Org. Chem.* **2004**, *69*, 8161.
(33) Molteni, C.; Parrinello, M. *J. Am. Chem. Soc.* **1998**, *120*, 2168.
(34) Lee, H.-S.; Tuckerman, M. E. *J. Chem. Phys.* **2006**, *125*, 154507.
(35) Lee, H.-S.; Tuckerman, M. E. *J. Chem. Phys.* **2007**, *126*, 164501.
(36) Murakhtina, T.; Heuft, J.; Meijer, E. J.; Sebastiani, D. *ChemPhysChem* **2006**, *7*, 2578.
(37) Kirchner, B.; Wennmohs, F.; Ye, S.; Neese, F. *Curr. Opin. Chem. Biol.* **2007**, *11*, 134.
(38) Lee, S. L.; Debenedetti, P. G.; Errington, J. R. *J. Chem. Phys.* **2005**, *122*, 204511. See also: Damm, W.; Frontera, A.; Tirado-Rives, J.; Jorgensen, W. L. *J. Comput. Chem.* **1997**, *18*, 1955.
(39) Kony, D.; Damm, W.; Stoll, S.; van Gunsteren, W. F. *J. Comput. Chem.*, **2002**, *23*, 1416.
(40) Taubert, S.; Konschin, H.; Sundholm, D. *Phys. Chem. Chem. Phys.* **2005**, *7*, 2561.
(41) (a) Cloran, F.; Zhu, Y.; Carmichael, I.; Serianni, A. S. *J. Am. Chem. Soc.* **2000**, *122*, 6435. (b) Stenutz, R.; Carmichael, I.; Widmalm, G.; Serianni, A. S. *J. Org. Chem.* **2002**, *67*, 949. (c) Zhu, Y.; Pan, Q.; Thibaudeau, C.; Zhao, S.; Carmichael, I.; Serianni, A. S. *J. Org. Chem.* **2006**, *71*, 466. (d) Zhao, H.; Pan, Q.; Zhang, W.; Carmichael, I.; Serianni, A. S. *J. Org. Chem.* **2007**, http://dx.doi.org/10.1021/jo0619884.
(42) Czernek, J.; Lang, J.; Sklenář, V. *J. Phys. Chem. A* **2000**, *104*, 2788.
(43) Malkina, O. L.; Hricovíni, M.; Bízik, F.; Malkin, V. G. *J. Phys. Chem. A* **2001**, *105*, 9188.
(44) Larsson, E. A.; Uliczny, J.; Laaksonen, A.; Widmalm, G. *Org. Lett.* **2002**, *4*, 1831.
(45) Roslund, M. U.; Klika, K. D.; Lehtilä, R. L.; Tähtinen, P.; Sillanpää, R.; Leino, R. *J. Org. Chem.* **2004**, *69*, 18.
(46) Curatolo, W.; Neuringer, L. J.; Ruben, D.; Haberkorn, R. *Carbohydr. Res.* **1983**, *112*, 297.
(47) Thrippleton, M. J.; Edden, R. A. E.; Keeler, J. *J. Magn. Reson.* **2005**, *174*, 97.

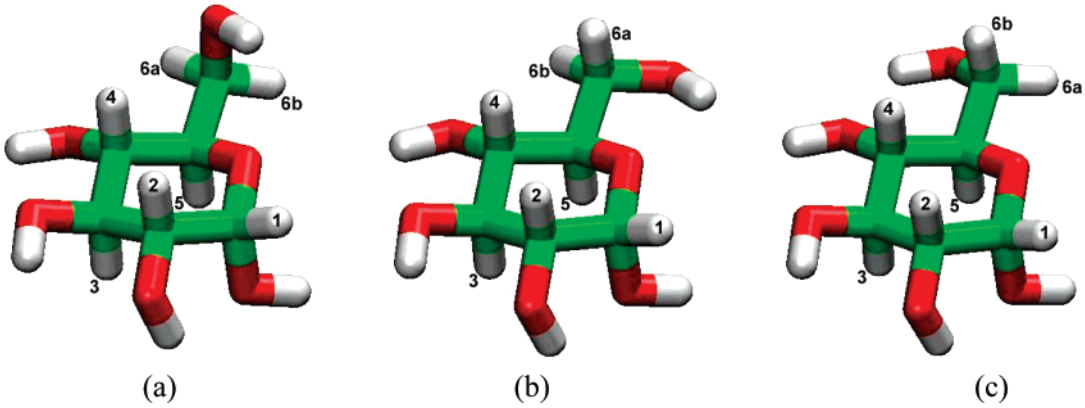

FIGURE 1. Optimized structures (gas phase, B3LYP/6-31G**) of the three rotamers *gg* (a), *gt* (b), and *tg* (c) with a counterclockwise arrangement of the intramolecular hydrogen bond chain.

TABLE 2. Experimental and Calculated (Gas Phase, B3LYP/cc-pVTZ//B3LYP/6-31G) ^{13}C and ^{1}H Chemical Shifts of α-D-Glucose**

	$\delta(^{13}C)$, ppm					$\delta(^{1}H)$, ppm				
	δ_{exptl}[a]	*gg*	*gt*	*tg*	avg[b]	δ_{exptl}[a]	*gg*	*gt*	*tg*	avg[b]
1	92.48	101.75	101.00	101.05	101.45	5.182	5.308	5.300	5.243	5.305
2	71.87	79.26	79.47	79.49	79.344	3.478	3.276	3.298	3.275	3.285
3	73.15	81.01	81.00	80.59	81.006	3.664	3.690	3.663	3.726	3.679
4	70.04	73.54	77.81	84.11	75.248	3.358	3.958	3.298	3.539	3.694
5	71.82	79.75	79.63	75.41	79.702	3.77	3.771	4.008	3.935	3.866
6a	60.99	64.83	68.65	72.65	66.358	3.711	4.021	3.572	3.724	3.841
6b						3.78	3.752	4.028	3.863	3.862
MAE		6.632	7.868	8.835	7.126		0.1847	0.1406	0.1097	0.1394
R^2[c]		0.9833	0.9999	0.8771	0.9936		0.8316	0.9461	0.9596	0.9393

[a] This work, see Table 1. MAE (mean absolute error) is defined as $(\sum_n|\delta_{calcd} - \delta_{exptl}|)/n$. [b] Calculated as $0.6\delta_{gg} + 0.4\delta_{gt}$ according to the population distribution. [c] Correlation coefficient of the linear fit $\delta_{calcd} = a + b\delta_{exptl}$.

conditions apply, which is the case for the (almost) isochronous protons 5 and 6b in α-D-glucose. In order to circumvent this issue, we have thus resorted to heteronuclear shift correlation spectroscopy. Due to the considerable signal crowding in the ^{13}C spectrum, a heteronuclear single-quantum correlation (HSQC) approach was preferred to its multiple-quantum counterpart (HMQC) since evolution of single-quantum coherences in the former pulse scheme is not modulated by homonuclear proton couplings and leads to a higher resolution of the indirect (^{13}C) dimension.[48] Experimental spectra are reported in the Supporting Information (Figures S1−S3).

Gas-Phase Calculations. Geometry optimizations have been carried out at the B3LYP level with the 6-31G** and 6-31+G** basis sets. The optimized structures, having the most stable counterclockwise arrangement of the hydroxyl hydrogen bonds,[26,27] are shown in Figure 1. Structure *tg* (c) corresponds to the minimum energy conformer in the gas phase, in agreement with previous studies, while structures *gg* (a) and *gt* (b) are calculated to be 0.4 and 0.7 kcal/mol higher, respectively (B3LYP/6-31G**).

We also tested the effect of adding diffuse functions since these have been claimed to be very important when dealing with carbohydrates.[31] Structures optimized with both 6-31G** and 6-31+G** basis sets have been used in the calculation of ^{13}C and ^{1}H chemical shifts; the cc-pVTZ or aug-cc-pVTZ basis sets have been correspondingly adopted, in keeping with our previous studies.[3,9,10] The results are collected in Tables 2 and S1.

In Figures 2 and 3, we show the correlation between the calculated and experimental ^{13}C and ^{1}H chemical shifts. For carbons, except for the *tg* conformer (not present in solution), a very good correlation is observed, although the calculated values are systematically overestimated by 5−10 ppm. Therefore, ^{13}C chemical shifts do not seem to be strongly affected by the structure and dynamics of the solvation shell of glucose. The *gt* conformer results appear in better agreement with experiment than the calculated values for *gg*. The effect of diffuse functions (Table S1) only amounted to a small systematic shift.

Concerning protons, significant differences are observed between the three rotamers; the population weighted average (60% *gg* + 40% *gt*) exhibits a significant discrepancy, more than 0.33 ppm, for H4 (δ_{calcd} = 3.694 ppm against δ_{exptl} = 3.358 ppm) and also a substantial deviation for H2 from the linear correlation, while the remaining protons are in rather good agreement. Interestingly, it is the *gg* conformer, the most abundant in solution, which shows the largest deviation of calculated H4 chemical shift, while the results of the *gt* conformer are, if taken alone, in reasonable agreement with the experiment. The strong deshielding of proton H4 in the *gg* conformer may be related to the close proximity of the lone pair of the hydroxymethylene oxygen. This effect should be significantly reduced in solution where the hydroxyl group is involved in hydrogen bonds with water.

The mean absolute error (MAE) amounts to 7.1 and 0.14 ppm for ^{13}C and ^{1}H, respectively. Whereas these statistical parameters look satisfactory in an absolute sense, the accuracy is not yet sufficient to assign all signals since the spacing of signals can be as small as 0.1 ppm (C2, C5) or 0.01 ppm (H5, H6b). Indeed, whenever two points in the correlation graph are connected by a segment with negative slope, the corresponding signals in the calculated spectrum are in incorrect order.[3]

(48) Mandal, P. K.; Majumdar, A. *Concepts Magn. Reson. A* **2004**, *20A*, 1.

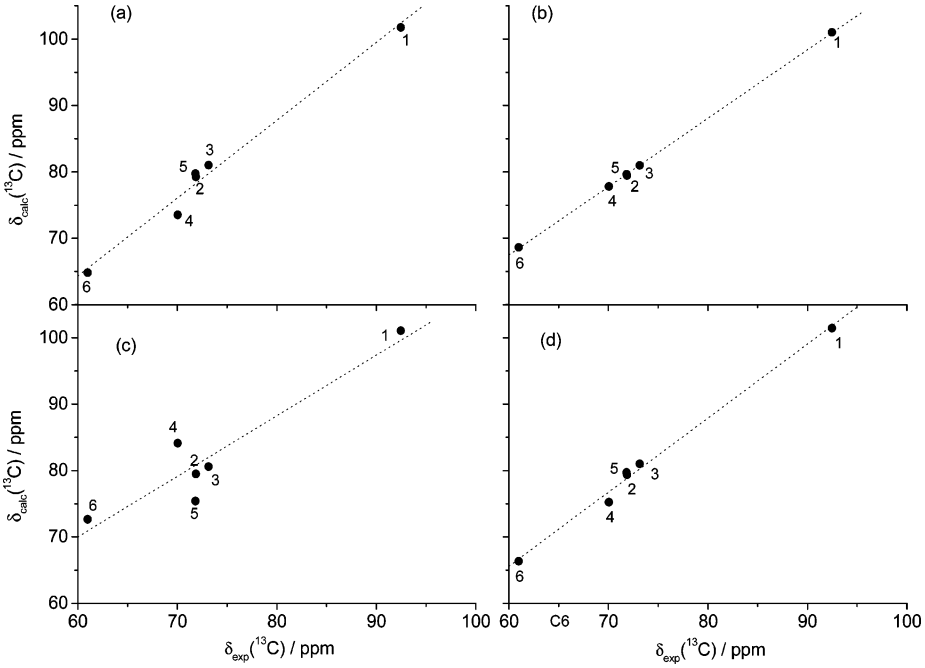

FIGURE 2. Correlation between calculated (gas phase, B3LYP/cc-pVTZ//B3LYP/6-31G**, see Table 2) and experimental ^{13}C chemical shifts of the rotamers of Figure 1: (a) *gg*; (b) *gt*; (c) *tg*; (d) weighted average (60% *gg* + 40% *gt*). Labels refer to atom numbers (Scheme 1). Linear fitting parameters, $\delta_{calcd} = a + b\delta_{exptl}$, of the weighted average results (d): $a = -1.3271$ ppm; $b = 1.1152$; $R^2 = 0.9936$. The best linear fit is shown as a dotted line (fitting parameters are reported in Table S3 of Supporting Information).

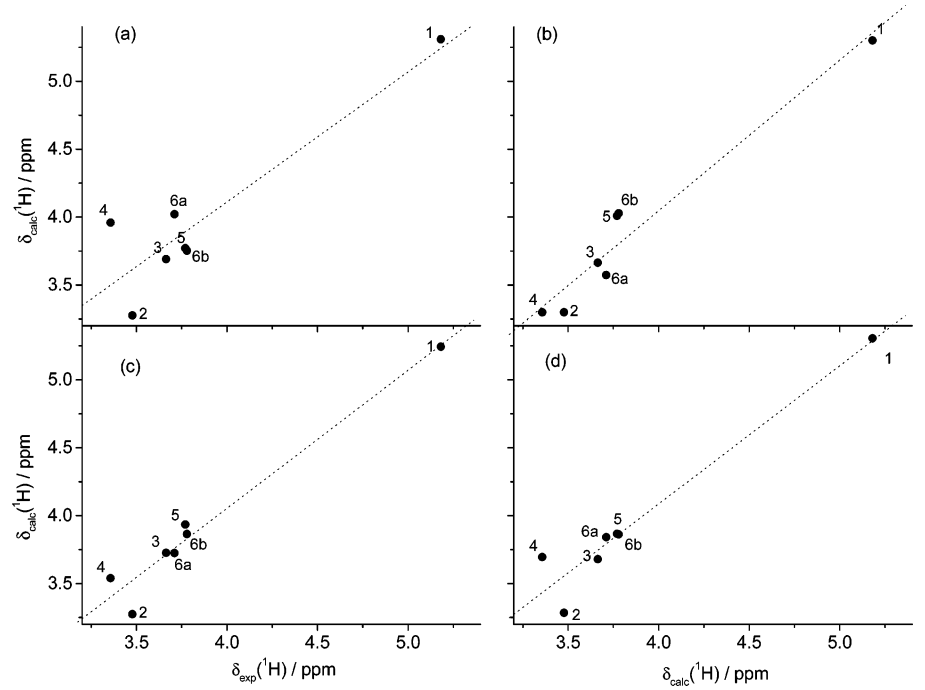

FIGURE 3. Correlation between calculated (gas phase, B3LYP/cc-pVTZ//B3LYP/6-31G**, see Table 2) and experimental ^{1}H chemical shifts of the rotamers of Figure 1: (a) *gg*; (b) *gt*; (c) *tg*; (d) weighted average (60% *gg* + 40% *gt*). Labels refer to atom numbers (Scheme 1). Linear fitting parameters, $\delta_{calcd} = a + b\delta_{exptl}$, of the weighted average results (d): $a = 0.0212$ ppm; $b = 1.0164$; $R^2 = 0.9393$. The best linear fit is shown as a dotted line (fitting parameters are reported in Table S3 of Supporting Information).

To understand the solvent effects, which appear to be important particularly for ^{1}H chemical shifts, we have undertaken a classical MD simulation of α-D-glucose in water (see Experimental Section). The results are presented in the next section. We have also calculated the shielding constants for the geometries optimized using the classical force field;[39] the results are reported in Figures S9, S10, and Table S2. The correlation is somewhat worse for ^{13}C but comparable to the DFT geometries for ^{1}H chemical shifts.

Molecular Dynamics Simulations. The rotamer distribution obtained in our 10 ns production run is a 73:23:4 *gg*:*gt*:*tg* ratio, close to the original result (69:27:4).[39] These results are in

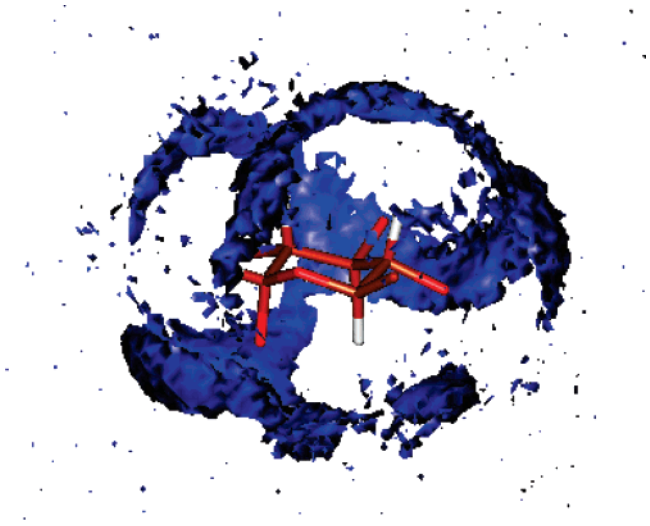

FIGURE 4. Spatial distribution function of the oxygen of water around glucose representing the probability of finding the oxygen atom of a water molecule at a given point in space around glucose. For clarity, the hydroxyl hydrogen and the hydroxymethylene hydrogen and oxygen atoms have been removed. This view shows the hydroxymethylene carbon and the ring oxygen at the forefront.

qualitative agreement with experiments, although the simulation predicts a somewhat higher stability for the *gg* conformer, compared with the experimental data.

Details of the simulations (time evolution and distribution function of the O5−C5−C6−O6 dihedral angle ϕ, radial distribution functions ($g(r)$) are reported in the Supporting Information (Figures S4−S7). Analysis of the various $g(r)$ confirms that strong hydrogen bonding occurs between water and the hydroxyl groups of glucose. In contrast, the probability density of water close to the alkyl hydrogen atoms is depleted compared to the bulk phase.

In Figure 4, we report the spatial distribution function of the oxygen of water around α-D-glucose. We note that the maximum probability, corresponding to the peaks in the $g(r_{OO})$ describing the distance between water oxygen and hydroxyl oxygen atoms, is shaped like a collar around the C−O axis of each hydroxyl oxygen.

Solution Phase Calculations. Ideally, in order to reliably compute chemical shifts in solution, one should run calculations that take into account all relevant factors, including structure and solvation effects.[12] However, the structure of a solvated system can hardly be determined by a DFT optimization of the solute embedded in a small cluster of solvent molecules because size effects and the flat potential energy surface will bias such calculations. For glucose, the situation is even more complicated, owing to the high flexibility of the solute. The workaround typically adopted averages the results of a series of DFT calculations run on snapshots taken from MD runs. Unfortunately, solute and solvent geometries are calculated empirically and hence may fall below the usual standards for NMR calculations. Thus, in order to (hopefully) separate structural and solvent effects, we have adopted an incremental approach in which emphasis is placed either on the solute or the solvent, as follows.

The MD trajectory has been used to extract a number of snapshots (one every 100 ps; see below) and, from each of these, a cluster containing either just the glucose molecule or glucose plus the first solvation shell of water molecules. Such clusters have been used for the QM calculation of glucose chemical shifts according to the following protocols. Shieldings have been calculated as averages over 50 (protocols a and b) or 100 snapshots (protocols c−f) extracted from the MD trajectory file, for a total of 500 DFT NMR runs. It is worth pointing out that the instantaneous fluctuations of the shielding constants may be as large as 2 ppm (Figure S8). However, convergence is essentially reached after only the first 50 configurations, so that convergence is ensured even for protocols a and b.

Unless specified otherwise, in shielding calculations, glucose was calculated at the B3LYP/cc-pVTZ level. In protocol a, we have only used the glucose molecule at the geometry resulting from the empirical force-field calculation without explicit water molecules, but including the solvent effect by means of the PCM continuum method. In protocol b, the glucose molecule was reoptimized at the B3LYP/6-31G** level before the calculation of the shielding constants, performed as in protocol a. Thus, these two protocols allow one to sample the conformations of the hydroxyl groups of glucose, in addition to the rotameric distribution, include the solvent reaction field and (in b) adopt a refined geometry for the solute, but do not include specific solvation effects. We remark that these optimizations do not converge to structures similar to those in the gas phase, that is, having an intramolecular network of hydrogen bonds; instead, glucose hydroxyl groups remain oriented in the same conformations they have in solution.

Remaining protocols c−f employed the geometry of glucose as obtained directly from MD with no further optimization and feature the treatment of solvent at various levels of sophistication (point charges and DFT, with or without reaction field). Thus, in c, we have included water molecules surrounding glucose up to 5.5 Å from the glucose center of mass (see Figure S5). While glucose is treated at B3LYP/cc-pVTZ, water molecules are modeled by point charges as defined in the force field.[49] In d, we have used a mixed basis set, BP86/TZ2P level for glucose and BP86/TZP.1s for water. Similarly, protocol e consists of glucose at B3LYP/cc-pVTZ plus water at B3LYP/6-31G** and PCM solvent; f same as d plus COSMO solvent.

When computed chemical shifts are derived from time averaging in solution, assigning a value to σ_{ref} is not straightforward, and this may hamper the determination of δ_{calcd} and hence of the MAE. It is possible to internally reference calculated shifts to an outstanding signal such as that of the anomeric proton.[18,19] However, this may lead to inconsistent results if the reference signal is itself subject to major variations, which is the case here. Therefore, we will evaluate the performance of each protocol mostly through the correlation coefficients. Calculated shielding constants and statistics are reported in Table 3, while the full statistical parameters are reported in Table S3.

In Figures 5 and 6, we show the correlation between calculated ^{1}H and ^{13}C shielding constants, protocol b, and experimental chemical shifts. The correlation graphs for the other protocols can be found in Figures S11 and S12 of Supporting Information. Note that in this case, since we compare the calculated shielding constants with the corresponding experimental chemical shifts, ideal correlation is represented by a straight line with a slope of −1.

(49) These calculations were run within the ONIOM scheme. See Karadakov, P. B.; Morokuma, K. *Chem. Phys. Lett.* **2000**, *317*, 589.

TABLE 3. Experimental Chemical Shifts and Calculated Shielding Constants (ppm) of ^{1}H and ^{13}C of α-D-Glucose in Water

		σ_{calcd}, ppm					
	δ_{exptl}, ppm[a]	a	b	c	d	e	f
H1	5.182	26.321	26.156	26.479	26.209	27.147	26.132
H2	3.478	28.127	27.991	28.187	27.819	28.760	27.753
H3	3.664	28.162	27.976	28.208	27.780	28.784	27.822
H4	3.358	28.389	28.143	28.382	28.020	28.979	28.003
H5	3.77	27.945	27.726	28.065	27.709	28.737	27.672
H6a	3.711	27.743	27.675	27.623	27.519	28.391	27.544
H6b	3.78	27.741	27.711	27.761	27.684	28.410	27.613
MAE[b]		0.1355	0.1363	0.1308	0.0695	0.1090	0.0810
R^2 [c]		0.9661	0.9872	0.9194	0.9770	0.9466	0.9774
C1	92.48	88.026	81.2714	87.498	88.275	91.523	88.870
C2	71.87	103.425	102.627	103.550	104.700	108.257	105.114
C3	73.15	104.402	100.777	104.617	105.757	108.484	105.555
C4	70.04	106.313	105.002	106.796	107.422	110.670	107.478
C5	71.82	109.002	103.696	108.923	108.996	111.977	109.411
C6	60.99	118.463	115.475	118.583	119.604	120.587	119.815
MAE[b]		2.281	1.115	1.847	1.591	2.029	1.918
R^2 [c]		0.9518	0.9968	0.9605	0.9682	0.9813	0.9647

[a] This work, see Table 1. See text for computational level pertaining to protocols a−f. [b] MAE (mean absolute error) is calculated as $(\sum_n|\delta'_{calcd} - \delta'_{exptl}|)/n$, where δ' is the chemical shift referenced to the anomeric proton and carbon (see text). [c] Correlation coefficient of the linear fit $\sigma_{calcd} = a + b\delta_{exptl}$.

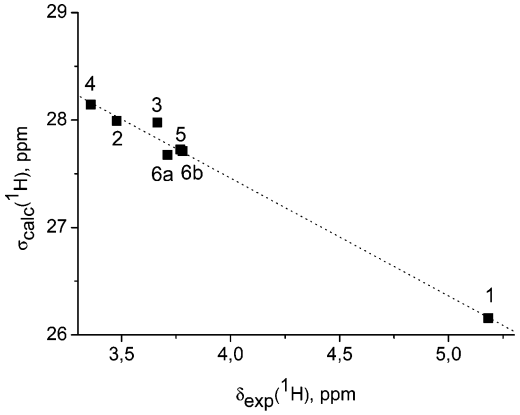

FIGURE 5. Correlation between calculated ^{1}H shielding constants (σ_{calcd}) and experimental chemical shifts (δ_{exptl}) for protocol b. The best linear fit is shown as a dotted line (fitting parameters are reported in Table S3 of Supporting Information).

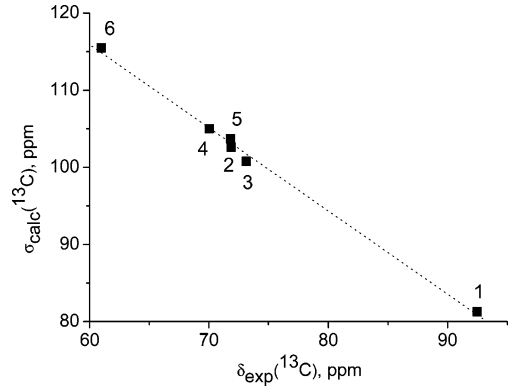

FIGURE 6. Correlation between calculated ^{13}C shielding constants (σ_{calcd}) and experimental chemical shifts (δ_{exptl}) for protocol b. The best linear fit is shown as a dotted line (fitting parameters are reported in Table S3 of Supporting Information).

Discussion

We will now evaluate the results, keeping in mind that the current accuracy of DFT methods is of the order of 0.1 ppm (^{1}H) or 1 ppm (^{13}C)[3] which is close to, or higher than, the spacing between adjacent signals.

One of the difficulties associated with the modeling of carbohydrate ^{1}H spectra is that most signals lie in a narrow region. This is clearly evident from Figure 5; the 0.5 ppm region between δ 3.3−3.8 ppm features all signals except H1. The latter is predicted to be the most deshielded by all methods, so we will concentrate on the critical H2−H6 signals, experimentally found in the sequence H4 < H2 < H3 < H6a < H5,6b.

All methods concur in predicting H4 and H2 to be the most shielded and in the correct order. The first difficulty comes with H3, which should lie 0.19 ppm downfield from H2. However, only protocols b and d arrange the signals correctly, albeit with a much smaller $\Delta\delta_{calcd}$ (0.01−0.04 ppm); in fact, all methods predict a very small difference.

On the contrary, the ordering and spacing between H3 and the next signal (H6a), 0.05 ppm, is always correctly modeled—except that this time the spacing is quite overestimated to ca. 0.3 ppm. This essentially interchanges H6a and the next signals (H5 and H6b), which differ by only 0.01 ppm. Notably, protocols b and d also predict H5 and H6b to have almost coincident chemical shifts, as required.

With regard to ^{13}C, and despite its well-known wide shift range, the overall situation is rather similar, with C1 strongly deshielded with respect to C2−C6. The latter signals span 12.2 ppm and are experimentally found in the order C6 < C4 < C2,5 < C3. Again, a critical issue is the extremely close spacing between C2 and C5 ($\Delta\delta_{exptl}$ = 0.05 ppm). The signals with highest spacing (C6, C4) are correctly predicted by all methods. On the other hand, only protocol b comes close to the correct prediction for C2,5 (however, with $\Delta\delta_{calcd}$ = 1.1 ppm). All others lead to C5 being much more shielded. Similarly, C3 is predicted to be more deshielded than C2 only by b.

In summary, protocol b definitely shows the best performance, which is also confirmed by the value of R^2, which is clearly superior for both ^{1}H and ^{13}C. The other statistical parameters, reported in Table S3, fully confirm this conclusion. In purely statistical terms, protocols d and f also perform similarly; however, the quality of those correlations is insufficient for this problem. It is worth noting that, compared to the gas phase, the inclusion of solvent effects as modeled in protocol b

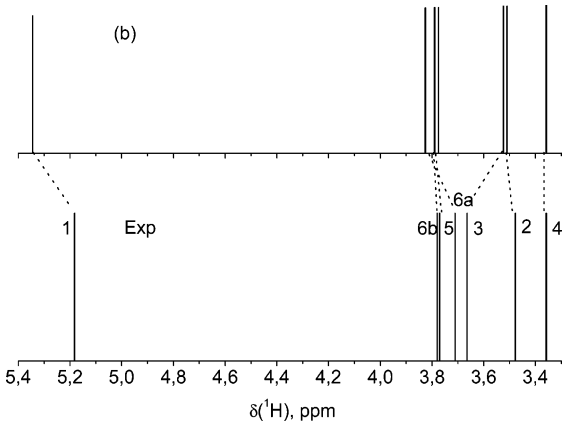

FIGURE 7. ^{1}H stick spectra of α-D-glucose in water. Top: results of protocol b. Bottom: experimental spectrum. The calculated spectrum has been shifted so that the most shielded signal, H4, matches the experimental one.

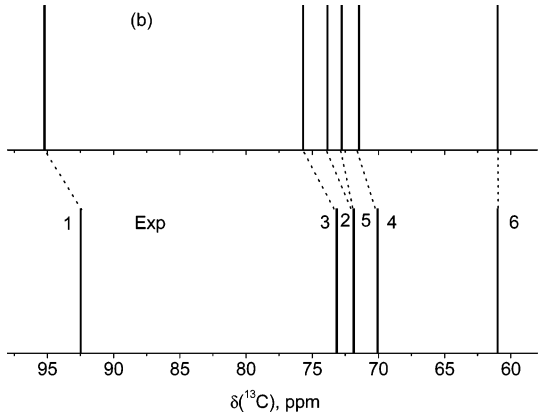

FIGURE 8. ^{13}C stick spectra of α-D-glucose in water. Top: results of protocol b. Bottom: experimental spectrum. The calculated spectrum has been shifted so that the most shielded signal, C6, matches the experimental one.

significantly improves the agreement for ^{1}H resonances (see Figures 5 and 3d) while retaining the high correlation of carbon resonances already obtained (see Figures 6 and 2d) because of the scarce solvent effect on ^{13}C chemical shifts.

We recall that protocol b is the only one where the geometry of glucose is optimized by DFT, but solvation is modeled only through the PCM continuum model; no explicit water molecules are considered. Thus, it seems that the most important factor determining the quality of computed shifts is the accuracy of the solute geometry. This is not too surprising since chemical shifts are very sensitive to geometrical parameters and a similar result was in fact reported in the seminal work of Malkin et al.[50] In the case of a conformationally flexible molecule such as glucose, however, this requirement must be matched by a representative sampling of its rotamers. A comparison with the only fair results of Figure 3d for ^{1}H highlights that such a sampling can only be achieved through an MD simulation *in solution*, rather than by explicit consideration of viable conformers. Indeed, the rigid arrangements that are found in the gas phase (regular cw or ccw for OH groups, *gg-gt-tg* for CH_2OH) are only a small subset of the conformations that are sampled by aqueous glucose; the simulation results of Figure 4 point out that (as one might have expected) water forms strong intermolecular hydrogen bonds, hence disrupting the intramolecular network portrayed in the gas phase.

The results are summarized, in a more visually appealing fashion, in Figures 7 and 8, where we show the stick spectra, ^{1}H and ^{13}C, respectively, based on the experimental and calculated chemical shifts.

Thus, the MD step serves the purpose of generating an acceptable sampling of solute conformations, as determined by both intra- and intermolecular interactions. However, because of the inherent limitations of classical nonpolarizable force fields, it does so only at the expense of the solute geometry being calculated at a rather low level—which is subsequently corrected by DFT optimization. We remark again that the DFT step cannot be consistently performed including a discrete solvation shell, but a solvent reaction field can be included.

It is then apparent that the worse performance of the other protocols stems from the use of the glucose geometry as obtained from MD snapshots. The inclusion of long-range solvent electrostatic effects through point charges (protocol c) is clearly insufficient (this method performs worst), whereas the improvement is noticeable if some explicit water molecules are included at a DFT level (albeit with the arrangement of the MD simulation, protocols d−f). Protocols e and f were expected to be superior, in that explicit solvent is supplemented with a PCM or COSMO reaction field; however, the changes are erratic, and no clear improvement is found.

Similar trends were observed in the case of other strongly solvated systems such as ionic liquids. The quality of their computed NMR spectra considerably improved upon going from classical[18] to Car−Parrinello simulations[19] as input for QM calculations, mostly because the latter afforded better geometries rather than because the dynamics were better described.

Conclusions

The solvent effect on the alkyl ^{1}H and ^{13}C chemical shifts is largely of indirect nature: the solvent affects the conformational distribution of the hydroxymethylene and hydroxyl groups which, in turn, affects the shielding constants. However, direct interaction of water molecules with glucose does not need to be explicitly included in the calculation of NMR properties. Although this may appear surprising, we note that we have been concerned only with carbon atoms which are exposed very little to the solvent and with alkyl hydrogen atoms which are not involved in strong interactions with water. Further support for this hypothesis is provided by a comparison of our data with ^{1}H and ^{13}C chemical shifts of glucose in water at 70 °C[51] where the water and the solvation dynamics are certainly different from that at room temperature. Nevertheless, at this higher temperature, all chemical shifts are only shifted systematically by 0.06 and 0.6 ppm, respectively, but the relative position is unaffected.

Experimental Section

NMR Spectra. NMR experiments were run at 600 MHz (^{1}H) and 150 MHz (^{13}C) with a 5 mm TXI *xyz* gradient inverse probe, at 298 K. The relevant spectral data for α-D-glucose were determined on a 10 mM D_2O solution of α-D-glucose equilibrated at room temperature for at least 48 h before use (both α and *β*

(50) Malkin, V.G.; Malkina, O.L.; Steinebrunner, G.; Huber, H. *Chem.—Eur. J.* **1996**, *2*, 452.

(51) Jansson, P.-E.; Kenne, L.; Schweda, E. *J. Chem. Soc., Perkin Trans. 1* **1988**, 2729.

anomers were present in the resulting sample). ^{1}H chemical shifts were obtained by combining results from DQF-COSY, double spin−echo (DSE) *J*-spectroscopy,[47] and sensitivity-enhanced HSQC spectroscopy.[52] ^{13}C chemical shifts were obtained directly from a power-gated ^{13}C spectrum, based on information retrieved from the HSQC map. Additional HSQC experiments were also run at 300 MHz (^{1}H) and 75 MHz (^{13}C). Experimental chemical shifts were referenced to TMS through the D_2O resonance frequency as measured by the lock channel. Digital resolution was 0.36 Hz for ^{1}H and 1.3 Hz for ^{13}C spectra.

QM Calculations. Geometry optimizations have been run using the hybrid B3LYP functional[53] with 6-31G** and 6-31+G** basis sets. NMR chemical shifts have been calculated at several levels of theory: with Gaussian03,[54] we used the B3LYP functional with cc-pVTZ (and aug-cc-pVTZ in the gas phase) basis sets for glucose and various levels of approximation for the solvent molecules as described in the text; the self-consistent reaction field model of solvation used was PCM.[55] Calculations with ADF[56] employed the non-hybrid GGA BP86 functional[57] with triple-ζ, single (TZP), or double polarized Slater basis sets (TZ2P) for water and glucose, respectively. For solvent water molecules, a slightly lower level of approximation was adopted; that is, in the TZP basis, the 1s shell was kept frozen in the SCF (TZP.1s). In this case, the continuum solvation model was COSMO.[58] For the gas-phase calculations, the chemical shift was obtained as $\delta = \sigma_{ref} - \sigma$, where σ_{ref} is the shielding constant of tetramethylsilane calculated at the same level of theory. When the shielding constant was calculated for clusters extracted from MD simulations, we compared the calculated shielding (σ_{calcd}) with the experimental chemical shift (δ_{exptl}). This is because a meaningful calculation of $\delta = \sigma_{ref} - \sigma$ can only be obtained when the two σ values are calculated at the same level of theory; this would require an MD simulation of the appropriate reference solute (TMS) in water to provide a number of clusters to be used for subsequent DFT calculations.

MD Simulations. The software MOSCITO has been used to run classical MD simulations.[59] The force field[39] is of OPLS-AA type and is specifically designed for the simulation of glucose in water. The parametrization introduces additional scaling factors for the electrostatic interactions between 1 and 5 and 1 and 6 atom pairs in order to reproduce the experimentally observed population of the rotamers of the hydroxymethyl group. The TIP3P water model was used, as in ref 35. OPLS rules were used to calculate mixed Lennard-Jones interaction parameters. Bond lengths were constrained by means of the SHAKE algorithm[60] with a tolerance of 10^{-4}. The smooth particle mesh Ewald summation has been used for long-range electrostatic interactions;[61] the short-range interaction cutoff radius was set at 8.0 Å. The integration scheme was the Verlet leapfrog algorithm with a time-step of 1 fs. The simulation was run in the NPT ensemble (using the weak coupling scheme of Berendsen et al.[62]) with a pressure of 0.1 MPa. The simulation box consisted of an α-D-glucose molecule plus 488 water molecules. The box was generated by first equilibrating a box of 512 TIP3P water molecules for 500 ps in the NPT ensemble, then adding the α-D-glucose molecule and removing the overlapping water molecules. The box was equilibrated for 500 ps in the NPT ensemble before the production run of 10 ns.

Acknowledgment. This work was financially supported by the University of Padova (Progetto di Ricerca di Ateneo CPDA045589). We thank Dr. W. Damm and Prof. W. F. van Gunsteren (ETH, Zürich) for sending us the parameter file of the modified force field of α-D-glucose.

Supporting Information Available: NMR spectra of α-D-glucose, Cartesian coordinates and computed energies of optimized structures, and radial distribution functions. This material is available free of charge via the Internet at http://pubs.acs.org.

JO071129V

(52) Schleucher, J.; Schwendinger, M.; Sattler, M.; Schmidt, P.; Schedletzky, O.; Glaser, S. J.; Sorensen, O. W.; Griesinger, C. *J. Biomol. NMR* **1994**, *4*, 301.

(53) (a) Becke, A. D. *J. Chem. Phys.* **1993**, *98*, 5648. (b) Lee, C.; Yang, W.; Parr, R. G. *Phys. Rev. B* **1988**, *37*, 785.

(54) Frisch, M. J.; Trucks, G. W.; Schlegel, H. B.; Scuseria, G. E.; Robb, M. A.; Cheeseman, J. R.; Montgomery, J. A., Jr.; Vreven, T.; Kudin, K. N.; Burant, J. C.; Millam, J. M.; Iyengar, S. S.; Tomasi, J.; Barone, V.; Mennucci, B.; Cossi, M.; Scalmani, G.; Rega, N.; Petersson, G. A.; Nakatsuji, H.; Hada, M.; Ehara, M.; Toyota, K.; Fukuda, R.; Hasegawa, J.; Ishida, M.; Nakajima, T.; Honda, Y.; Kitao, O.; Nakai, H.; Klene, M.; Li, X.; Knox, J. E.; Hratchian, H. P.; Cross, J. B.; Bakken, V.; Adamo, C.; Jaramillo, J.; Gomperts, R.; Stratmann, R. E.; Yazyev, O.; Austin, A. J.; Cammi, R.; Pomelli, C.; Ochterski, J. W.; Ayala, P. Y.; Morokuma, K.; Voth, G. A.; Salvador, P.; Dannenberg, J. J.; Zakrzewski, V. G.; Dapprich, S.; Daniels, A. D.; Strain, M. C.; Farkas, O.; Malick, D. K.; Rabuck, A. D.; Raghavachari, K.; Foresman, J. B.; Ortiz, J. V.; Cui, Q.; Baboul, A. G.; Clifford, S.; Cioslowski, J.; Stefanov, B. B.; Liu, G.; Liashenko, A.; Piskorz, P.; Komaromi, I.; Martin, R. L.; Fox, D. J.; Keith, T.; Al-Laham, M. A.; Peng, C. Y.; Nanayakkara, A.; Challacombe, M.; Gill, P. M. W.; Johnson, B.; Chen, W.; Wong, M. W.; Gonzalez, C.; Pople, J. A. *Gaussian 03*, revision B.05; Gaussian, Inc.: Pittsburgh, PA, 2003.

(55) (a) Cancès, M. T.; Mennucci, B.; Tomasi, J. *J. Chem. Phys.* **1997**, *107*, 3032. (b) Cossi, M.; Barone, V.; Mennucci, B.; Tomasi, J. *Chem. Phys. Lett.* **1998**, *286*, 253. (c) Mennucci, B.; Tomasi, J. *J. Chem. Phys.* **1997**, *106*, 5151. (d) Cossi, M.; Scalmani, G.; Rega, N.; Barone, V. *J. Chem. Phys.* **2002**, *117*, 43.

(56) te Velde, G.; Bickelhaupt, F. M.; Baerends, E. J.; Fonseca Guerra, C.; van Gisbergen, S. J. A.; Snijders, J. G.; Ziegler, T. *J. Comput. Chem.* **2001**, *22*, 931.

(57) (a) Becke, A. D. *Phys. Rev. A* **1988**, *38*, 3098. (b) Perdew, J. P. *Phys. Rev. B* **1986**, *33*, 8822.

(58) (a) Pye, C. C.; Ziegler, T. *Theor. Chem. Acc.* **1999**, *101*, 396−408.(b) Klamt, A.; Schüürmann, G. *J. Chem. Soc., Perkin Trans. 2* **1993**, 799. (c) Klamt, A. *J. Phys. Chem.* **1995**, *99*, 2224. (d) Klamt, A.; Jones, V. *J. Chem. Phys.* **1996**, *105*, 9972.

(59) *MOSCITO 4*, Paschek, D.; Geiger, A. Department of Physical Chemistry, University of Dortmund, 2002.

(60) Ryckaert, J. P.; Ciccotti, P.; Berendsen, H. J. C. *J. Comput. Phys.* **1997**, *23*, 327.

(61) Essmann, U.; Perera, L.; Berkowitz, M. L.; Darden, T.; Lee, H.; Pedersen, L. G. *J. Chem. Phys.* **1995**, *103*, 8577.

(62) Berendsen, H. J. C.; Postma, J. P. M.; van Gunsteren, W. F.; Di, Nola, A.; Haak, J. R. *J. Chem. Phys.* **1984**, *81*, 3684.